WAKEFIELD OF TWO COUNTER-ROTATING BEAMS

L. Teofili[1,2], M. Migliorati*[1,2], Sapienza University of Rome, Rome, Italy
I. Lamas, CERN, Geneva, Switzerland
[1]also at CERN, Geneva, Switzerland, [2]also at INFN, Rome, Italy

Abstract

This paper deals with the problem of defining the wakefunction for two counter-moving charges, i.e. two charges moving in opposite direction. In this case, the distance between the charges cannot be considered constant. From the counter-moving wakefunction the counter-moving wakepotential is derived. An example of this kind of wakepotential for a lossless pill-box cavity is obtained analitically and compared with numerical simulations.

INTRODUCTION

During their motion in an accelerator, the beam particles interact electromagnetically with the accelerator vacuum chamber generating the so-called wakefields. These wakefields dissipate heat on the vacuum chamber materials (RF-heating) and act back on the beam particles triggering instabilities. In the case of a single beam traversing the vacuum chamber all the particles move in the same direction and this could be defined as co-moving wakefield [1] or simply wakefield (refer to Fig. 1a).

The physical model for quantifying the effects of the co-moving wakefield has been object of studies since many years, and the works of Chao [2], Ng [3], Bane et al. [4] are well known examples of the current understanding on the topic.

However, in particle colliders there is an extra complication due to the presence of two counter-rotating particle beams. Usually, the two beams pass in two separate vacuum chambers. However, in the collision regions and, sometimes, also in other components, they transit in the same vacuum chamber. In this case, the particles of one beam move in opposite direction with respect to the particles of the other beam and one talks about counter-moving wakefield [1], (refer to Fig. 1b).

In particular, in the Large Hadron Collider (LHC) [5] at the laboratories of the European Council for Nuclear Research (CERN) two counter-rotating beams circulate. They transit in the same vacuum chamber in the collision chambers, at the four interaction points, and in few other components as the LHC injection absorber also known with the acronyms TDI [6] (Target dump injection) which is the device currently installed and TDIS [7] (Target dump injection segmented) which is the upgrade of the TDI to be installed in 2020.

The TDI had major issues due to unexpected severe RF-heating [8] still not fully understood. A possible explanation could be linked to the RF-heating resulting from the interaction of the two counter-rotating beams. In order to avoid these issues with the TDIS, CERN allocated resources to investigate the counter-rotating beam effects.

Few studies have investigated the interaction between two counter-moving beams via their wakefield[1]: Pellegrini [10] and Wang [1] studied longitudinal and transverse two-beam instabilities linked to resonant modes for the Large Electron Positron storage ring (LEP) [11]. Zimmerman [12] discussed the resistive wall wakefield problem for two counter-moving beams. Zannini et al. [13, 14] and Grudiev [15] focused on the RF-heating induced in a vacuum chamber traversed by the counter-moving beams.

This paper proposes a formal physical model to describe the counter-moving wakefield effects starting from the wakefield hypotheses. It defines a counter-moving wakefunction for two point charges, a source charge S and a test charge T. The counter-moving and co-moving cases are represented in Fig. 1. In this figure, most of the quantities needed for understanding the paper are presented.

The paper introduces also the counter-moving wakepotential. Furthermore, it benchmarks the model against simulations results for a lossless cylindrical resonant cavity. Future works will test the model to re-obtain the results of Wang, [1], Zimmerman [12], Zannini et al. [13, 14] and Grudiev [15].

THE PHYSICAL MODEL

The approximations on which the definition of wakefield is based are two [3]:

1. **Rigid Beam Approximation.** The trajectories of S and T are given, they are straight and parallel with each other. Furthermore, the speed modulus of T and S is equal and constant $v_{qS} = \beta_{qS} c = v_{qT} = \beta_{qT} c = v$ while the two particles traverse the vacuum chamber.

2. **Kick Approximation.** The effects of the electromagnetic force, continuously acting on S and T all along the vacuum chamber, are represented as a lumped kick acting after the particles passage.

Often in the literature the first hypothesis is reformulated as follows: the trajectories of S and T are given, they are straight and parallel with each other and the longitudinal relative position of T with respect to S (represented as s_{ST} in Fig. 1) during the particle transit in the vacuum chamber is constant, i.e. time-independent.

The authors want to stress that this is not the rigid beam approximation but only one of its consequences. The time

* mauro.migliorati@uniroma1.it

[1] This is not to be confused with the Beam-Beam interaction [9] that does not consider the beams environment.

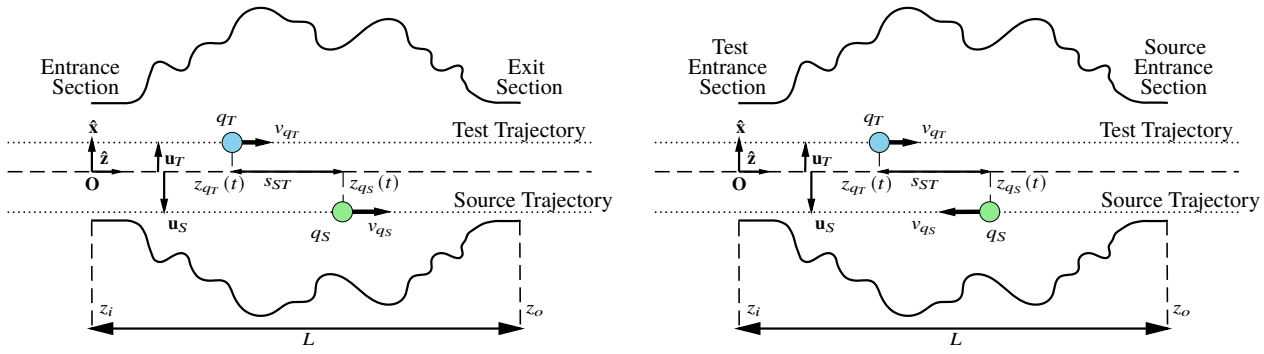

(a) Co-moving case, S and T move in the same direction.

(b) Counter-moving case, S and T move in opposite direction.

Figure 1: Source (q_S) and Test (q_T) charge transiting inside a vacuum chamber. The cartoon underlines the instantaneous z positions of the two charges $z_{qS}(t)$ and $z_{qT}(t)$, their speeds v_{qS} and v_{qT}, their longitudinal distance $s_{ST}(t)$ and the transverse position of their trajectories with respect to the main reference frame $\mathbf{u}_T$ and $\mathbf{u}_S$. The fixed reference system $\mathbf{O}$, with origin in the entrance section of the test particle and the $\hat{\mathbf{z}}$ axis aligned with the test particle velocity vector. The length of the vacuum chamber L is also indicated.

independence of the relative position of T with respect to S can be derived from the rigid beam approximation adding the extra hypothesis that T and S move in the same direction (co-moving case). The rigid beam approximation, as stated in this paper, remains valid also if the relative positions between the particles is changing inside the vacuum chamber. This is the case for the counter-moving wakefield scenario where the particle distance s_{ST} changes while T and S are traversing the vacuum chamber, i.e. s_{ST} is time dependent (refer to Fig. 1b).

The physical formal model that describes quantitatively the effects of the wakefield is well known and tested for the co-moving case. The interested reader can refer for instance to the work of Chao [2] for more detail. However, this model relies on the time independence of the longitudinal test source distance s_{ST}.

If one considers the counter-moving case the longitudinal test source distance s_{ST} is not constant any more and the formal model used for the co-moving case is not applicable as it is. However, it can be adapted as it is explained in the following.

Primarily, one notes that there is a time delay between the entrance in the vacuum chamber of the source charge S and of the test charge T. This time entrance delay is defined as:

$$\Delta t_{ST} = t_{Ti} - t_{Si}, \tag{1}$$

where t_{Ti} is the entrance time of the test particle into the vacuum chamber and t_{Si} is the entrance time of the source particle into the vacuum chamber. For the sake of clarity, the test particle enters into the vacuum chamber when crosses the Test Entrance Section, while the source particle enters into the vacuum chamber when crosses the Source Entrance Section, (see Fig. 2).

One defines also the space entrance delay as the distance that T has to cover to enter into the vacuum chamber at the

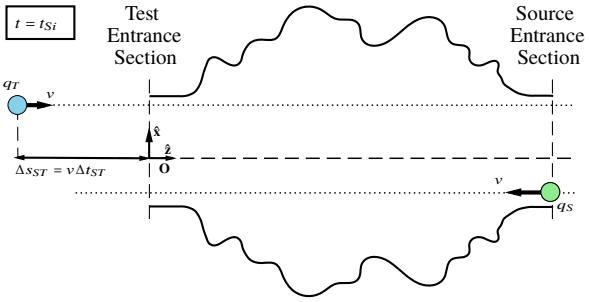

Figure 2: Counter-moving Wakefield scenario. The cartoon represents the position of S and T at the time at which the source is entering into the vacuum chamber, t_{Si}. The space entrance delay Δs_{ST} is also represented, it is the distance that T has to cover to enter into the vacuum chamber at the time at which S is entering.

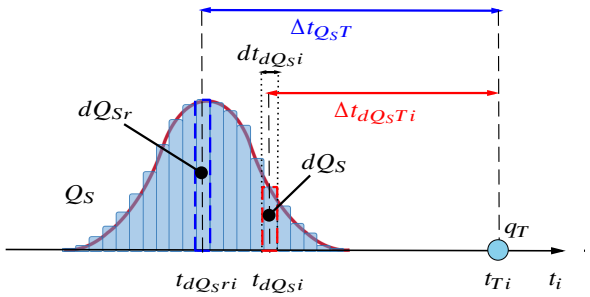

Figure 3: Representation of the charge distribution Q_S and of the test charge q_T as a function of their entrance time into the vacuum chamber t_i. In the picture t_{dQSi} is the entrance time of dQ_S, the generic infinitesimal charge composing the distribution Q_S, t_{dQSri} is the entrance time of dQ_{Sr}, the reference infinitesimal charge of the distribution Q_S. The entrance time delay of the test charge q_T with respect with this two charges, Δt_{ST} and Δt_{QST} is also shown.

time at which S is entering into the vacuum chamber :

$$\Delta s_{ST} = \Delta t_{ST} v, \tag{2}$$

where v is the particles speed. The authors want to stress that, in the co-moving case the space entrance delay is coincident with the longitudinal distance between T and S and the concepts of time entrance delay, space entrance delay and longitudinal particle distance are equivalent. This is not the case in the counter-moving scenario.

Subsequently, one has to recall the physical meaning of the wakefunction: the wakefunction represents the integrated effect (change of energy in the longitudinal direction and change of transverse momentum in the transverse plane) that the electromagnetic field excited by the transit of the source charge S in the vacuum chamber has on the test charge T that enters the vacuum chamber with a time delay Δt_{ST} with respect to S.

Thus, the counter-rotating wakefunction is defined as:

$$\begin{aligned}\mathbf{w}(\mathbf{u}_T, \mathbf{u}_S, \Delta t_{ST}) = &\frac{1}{q_S q_T} \\ &\times \int_{t_{Ti}}^{t_{To}} \mathbf{F}(\mathbf{u}_T, \mathbf{u}_S, \Delta t_{ST}, t) v dt,\end{aligned} \tag{3}$$

where, $\mathbf{F}$ is the instantaneous Lorentz force acting on T and t_{To} is the exit time of the test particle from the vacuum chamber. The counter-rotating wakefunction $\mathbf{w}$ defined by Eq. 3 is a vector of three components, the component along the $\hat{\mathbf{z}}$ axis is called longitudinal and the other two transverse. Further, the definition of wakefunction given by Eq. 3 is general and can be used for both the co-moving and counter-moving cases.

From the counter-moving wakefunction one can pass to the counter-moving wakepotential considering the source as a charge distribution $Q_S(t) = q_S \lambda_S(t)$ composed by slices of charge dQ_S. Each slice of charge can be thought as a point charge that enters into the vacuum chamber at a time t_{dQSi} and has a different entrance delay with respect to the test charge. The charge of each slice can be expressed as $dQ_S(t_{dQSi}) = q_S \lambda_S(t_{dQSi}) dt_{dQSi}$. It is also useful to define Δt_{QST}, the time entrance delays between the source distribution Q_S and the test charge T, as the entrance delay between the test charge and a reference slice in the distribution (as for instance the slice with the highest charge). The space entrance delay between the source distribution Q_S and the test charge T, Δs_{QST}, follows from the time entrance delay as: $\Delta s_{QST} = v \Delta t_{QST}$.

A visualization of these quantities is given in Fig. 3. The figure represents the sliced charge distribution Q_S and the test charge q_T as a function of their entrance time into the vacuum chamber t_i.

Finally, the counter-moving wakepotential is defined as the convolution between the wakefunction $\mathbf{w}$ and the normalized charged distribution λ_S:

$$\begin{aligned}\mathbf{W}(\mathbf{u}_S, \mathbf{u}_T, t_{Ti}) = &\int_{-\infty}^{\infty} \lambda_S(t_{dQSi}) \\ &\times \mathbf{w}(\mathbf{u}_T, \mathbf{u}_S, t_{Ti} - t_{dQSi}) dt_{dQSi}.\end{aligned} \tag{4}$$

The longitudinal component of Eq. 4 can be used to obtain an expression of the energy gained or lost by the test particle, however, this topic will be discussed in future works.

EXAMPLE: PILL-BOX CAVITY

This section gives an example of counter-moving longitudinal wakepotential for the case of a lossless pill-box cavity. The wakefunction is obtained semi-analytically integrating the expression of the longitudinal electric field generated by a short burst disk of electrons emitted by one side of the cavity that travels towards the other side at a speed v_S, refer to Fig. 4. The wakefunction is subsequently convolved with a Gaussian bunch distribution to obtain the wakepotential. This wakepotential is benchmarked against the results of the PIC solver [16] of the CST studio suite commercial software.

The analytic expression of transient longitudinal electric field generated by a disk of electrons moving from one side of a pill-box cavity of radius a and length L, and that travels towards the other side at a speed $v_S = \beta_S c$, was found by Faust [17] as:

$$\begin{aligned}E'_z(r'_{qT}, z'_{qT}, t) = &-\frac{eN}{\epsilon_0}\left\{\frac{\beta_S}{L}\left[ctU(ct) - \left(ct - \frac{L}{\beta_S}\right)U\left(ct - \frac{L}{\beta_S}\right)\right] - U\left(ct - \frac{z'_{qT}}{\beta_S}\right) - \ldots\right. \\ &- \frac{2a\beta_S}{L}\sum_{m=1}^{m=\infty}\frac{J_0(r'_{qT}\rho_m/a)}{J_1(\rho_m)\rho_m^2}\left[\sin\left(\rho_m\frac{ct}{a}\right) - \sin\left(\rho_m\frac{ct - L/\beta_S}{a}\right)U\left(ct - \frac{L}{\beta_S}\right)\right] - \ldots \\ &- \frac{4a\beta_S}{L}\sum_{m=1}^{m=\infty}\sum_{n=1}^{n=\infty}\frac{J_0(r'_{qT}\rho_m/a)}{J_1(\rho_m)}\rho_m \cdot \frac{\sin(\gamma_1 ct/a) - (-1)^n \sin(\gamma_1\frac{ct-L}{\beta_S a})U\left(ct - \frac{L}{\beta_S}\right)}{\gamma_1\gamma_2^2}\cos\left(\frac{n\pi z'_{qT}}{L}\right) + \ldots \\ &\left. + \frac{2}{\pi}\sum_{n=1}^{n=\infty}\frac{I_0(r'_{qT}n\pi\gamma_S/L)}{nI_0(an\pi\gamma_S/L)}\left[\sin\left(n\pi\beta_S\frac{ct}{L}\right) - (-1)^n\sin\left(n\pi\beta_S\frac{ct - L/\beta_S}{L}\right)U\left(ct - \frac{L}{\beta_S}\right)\right]\cos\left(\frac{n\pi z'_{qT}}{L}\right)\right\},\end{aligned} \tag{5}$$

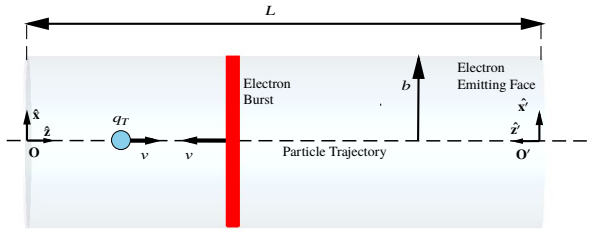

Figure 4: Pill-Box cavity excited by an electron burst emitted from one of the circular faces, counter-moving case scenario. Note that in this case the reference frame in which the wakefunction is needed, **O**, and the reference frame in which Eq. 5 gives the electric field, **O′**, are not coincident.

where, N is the number of electrons per square meter, $J_0(x)$ is the Bessel function of order zero, ρ_m are the roots of the Bessel function J_0, $I_0(x)$ is the modified Bessel function of order zero, $U(t)$ is the unit function, $\gamma_S = 1-\beta_S^2$, $\gamma_1^2 = \rho_m^2 + (n\pi a/L)^2$ and $\gamma_2^2 = \rho_m^2 + (n\pi a)^2(1-\beta_S^2)/L^2$. Furthermore, $r_{q_T}(t)'$ and $z_{q_T}(t)'$ are the generic radial and longitudinal position of a test particle T in a reference frame **O′** with origin in the electron emission face and $\hat{\mathbf{z}}'$ oriented in the direction of motion of the electrons. The electric field E_z' given by Eq. 5 is also expressed in the **O′** reference frame. Finally, t is the generic time. Considering the expression of the electric field in the device as a function of time, it is possible to compute the counter-moving wakefunction.

The geometry of the problem is drawn in Fig. 4. In the counter-rotating wakefield case the reference frame in which the wakefunction is defined, **O**, is not the same as that in which the longitudinal electric field of the electron disk is given by Eq. 5, **O′**. Indeed **O** has its origin in the test entrance section and its $\hat{\mathbf{z}}$ axis points in the direction of motion of T while **O′** has its origin in the source entrance section and its $\hat{\mathbf{z}}'$ axis points in the direction of motion of the electron burst, that is opposite to the one in which T is moving in the counter-rotating case, refer to Fig. 4. The quantities in **O′** are linked to the quantities in the **O** by the following equations:

$$\begin{aligned} r'_{q_T} &= r_{q_T} \\ z'_{q_T} &= L - z_{q_T} \\ E'_z &= -E_z. \end{aligned} \tag{6}$$

Considering Eq.s 6, the first two equations can be intuitively derived looking at Fig. 4, where both reference frame **O** and **O′** are represented. The third relation is true because the z axes of the two frames point in opposite directions. Thus, if E_z is positive in one of the frames, **O** for example, i.e. E_z is directed as the z, it is naturally negative in the other, **O′**, i.e. E_z is directed against $\hat{\mathbf{z}}$.

If $t = 0$ is chosen as the time at which the electron disk leaves the emitting face, the relation $z_{q_T}(t) = vt - \Delta s_{ST}$ holds as equation of motion of T. Substituting this relation into Eq.s 6 one has:

$$\begin{aligned} r'_{q_T} &= r_{q_T} \\ z'_{q_T} &= L - vt + \Delta s_{ST} = L - vt + v\Delta t_{ST} \\ E'_z &= -E_z, \end{aligned} \tag{7}$$

where, $v = v_S = v_T$ and Eq. 2 were used.

The counter-moving wakefunction is defined in a reference frame with the longitudinal axis towards the direction of motion of T, the **O** frame in this case. Thus, using Eq.s 7 into the expression of the longitudinal electric field, Eq. 5, the electric field can be rewritten in the wanted frame (**O**) as a function of time and entrance delay.

Once the electric field is know in the **O** frame, the longitudinal counter-moving wakefunction can be computed using Eq. 3. Note that only the electric field play a role in the Lorentz force along the direction of motion.

To obtain the counter-moving wakefunction one has to recall that, since $t = 0$ has been chosen as the time at which the source electron burst is emitted from the cavity surface, Δt_{ST} represents also the time at which T enters into the pillbox cavity, thus: $t_{Ti} = \Delta t_{ST}$ and $t_{To} = t_{Ti} + \frac{L}{v}$. The last one of the previous relations is true because of the rigid beam approximation.

This process was repeated to compute also the longitudinal co-moving wakefunction. To do so, Eq. 3 was used and the longitudinal electric field acting on the test charge was computed using Eq. 5, considering the following relations instead of the Eq.s 6 and 7: $r'_{q_T} = r_{q_T}$, $z'_{q_T} = z_{q_T} = vt - v\Delta t_{ST}$, $E_z = E'_z$. These relations hold because in the co-moving case the reference systems **O** and **O′** are coincident, i.e. they have the same origin (the electron emission face that is also the entrance section of T) and their corresponding axis are oriented in the same way.

The co and counter-moving wakefunctions were numerically evaluated for the case in which both the electrons and the test particle are ultra-relativistic, i.e. $\beta_S = 1$ and $v = c$. As a function of the entrance delays, they are reported in Fig. 5 and their Fourier Transforms, the co and counter-moving impedance, in absolute values, are reported in Fig. 6.

Unfortunately, the real and imaginary part of the co-moving and counter-moving impedance were affected by high noise, thus, in this paper, a comparison of the real and imaginary part of the co-moving and counter-moving impedance is not reported. This comparison is left for future work.

To obtain the wakepotential, the wakefunction was numerically convolved with a beam distribution λ_S. The considered beam distribution was Gaussian.

To benchmark the validity of the calculations, numerical simulations were performed. Using the Particle in Cell (PIC) solver of CST, the excitation of a loss free pillbox (length L = 0.6 m and radius a = 0.1 m) by a burst of electrons emitted by one of the circular face was simulated. The cavity material was set to be perfect electric conductor (PEC), so that the cavity was loss free. The electrons were emitted uniformly from the face with a Gaussian longitudinal distribution (σ_b =

0.07 m). One bunch of electrons with a total charge of 1 nC ($6.24 \cdot 10^9$ electrons) was emitted. The kinetic energy of the electrons was set to an ultra-relativistic value ($\gamma = 5 \cdot 10^{10}$) to avoid space charge effects. The total simulation time was set to 20 ns, electric field monitors were set to register and store the value of the longitudinal electric field every 1.5 mm along the whole cavity axis, that is every $5 \cdot 10^{-3}$ ns. The position of the test particle T is known at every time t as a function of the entrance delay ($z_{q_T}(t) = vt - \Delta s_{ST} = vt - v\Delta t_{ST}$), i.e. fixing an entrance delay Δs_{ST} or Δt_{ST}, one knows the T longitudinal position z_{q_T} at the time t. If z_{q_T} at the time t is known, one can obtain the value of the longitudinal electric field acting on T at the time t from the fields monitors. If this operation is repeated for every t one obtains the longitudinal electric field experienced by T traversing the cavity as a function of time (or equivalently as a function of its longitudinal position). Integrating this longitudinal electric field one has the wakepotential value for the set entrance delay, and repeating the integration for different entrance delays gives the whole wakepotential.

The counter-rotating wakepotentials as a function of the entrance delay between Q_S and T ($\Delta s_{Q_S T}$ and $\Delta t_{Q_S T}$) obtained from the formal model and the CST PIC solver are reported and compared in Fig. 7. The agreement between the two methods is excellent.

DISCUSSION

In Fig. 5 the co-moving and counter-moving wakefield and wakepotential for a pill-box cavity excited by a burst of electrons were presented and compared.

Further, in Fig. 6, the co-moving and counter-moving longitudinal impedance are reported.

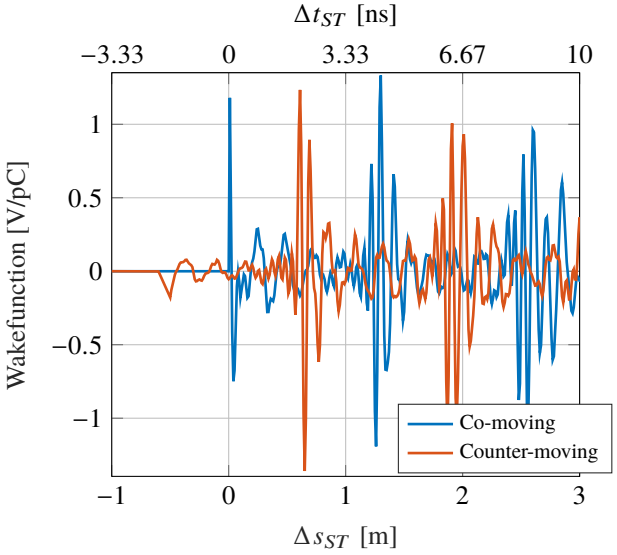

Figure 5: Comparison between the co-moving and the counter-moving wakefunction of a pill box cavity excited by a burst of electrons emitted by one of the faces. The wakefunctions have been obtained with the Faust theory.

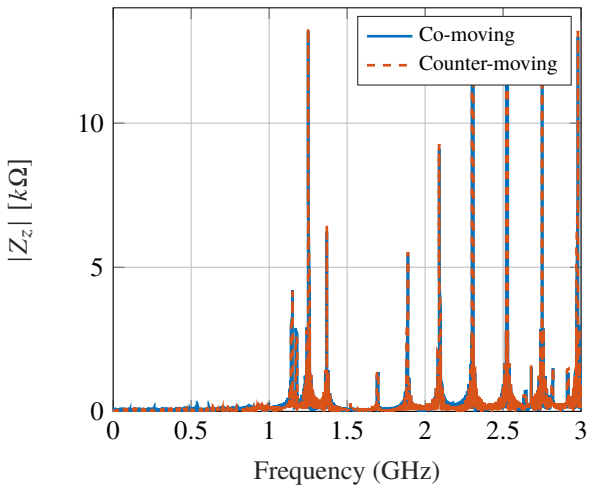

Figure 6: Comparison between the co-moving and the counter-moving impedance of a pill box cavity excited by a burst of electrons emitted by one of the faces.

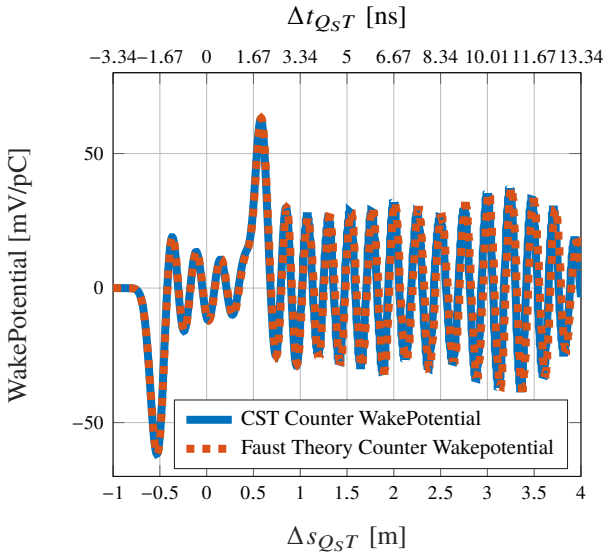

Figure 7: Comparison between the counter-moving wakepotentials of a burst of ultra-relativistic electrons (1 nC or $6.24 \cdot 10^9$ electrons and $\beta_S \to 1$ or $\gamma_S = 5 \cdot 10^{10}$) traversing a pill box cavity (length $L = 0.6$ m and radius $a = 0.1$ m) computed by the proposed model (Using the Faust Theory [17]) and the CST PIC solver [16]. The electrons are emitted uniformly from one of the circular faces of the cavity. Their longitudinal distribution is a Gaussian bunch ($\sigma_b = 0.07$ m). The cavity material is perfect electric conductor (PEC), loss free. Test particle speed is $v = c$.

Let us label as transient the interval of time for which the source particle is inside the cavity, ($\Delta s_{ST} < 0.6$ m for the discussed example), and as long range interval the period of time after the transient, i.e. $\Delta s_{ST} > 0.6$ m.

With reference to Fig. 5, co-moving and counter-rotating wakefunction are different in the transient region, around null entrance delay between T and S, while for further entrance delay they seem to be similar but translated. This indicates that the effects of the transient wakefield generated by S is experienced in a very different way if T moves in the same (co-moving wake) or in opposite (counter-moving) direction with respect to S. However, it appears that the effects of the long range wakefield generated by S are quite similar in both the co-moving and the counter-moving case. This makes sense since the long range interval is dominated by the resonant electromagnetic modes trapped in the pill-box, and the geometry of the mode fields and the mode resonant frequency is invariant with respect to the direction of the test particle. This last observation is backed up by the fact that, co-moving and counter-moving longitudinal impedance modulus compare very well, refer to Fig. 6, i.e. the resonant modes have similar effects on the test charge T independently from its propagation direction.

Finally, Fig. 7 compares the counter-moving wakepotential obtained using the proposed physical model (with the Faust equations) and the CST PIC solver simulations. There is an excellent agreement between the results of the proposed model and the results of the simulations. This can be thought both as a first benchmark for the proposed model, and for the CST software.

CONCLUSION

This paper has introduced a physical model to define and quantify the wakefunction of two particle moving in opposite directions. The paper has first reviewed the two approximations on which the co-moving wakefunction definition is based, and it has been observed that they can be used also in the counter-moving case. Furthermore, the paper has introduced the concept of space and time entrance delay. Using them, a coherent physical model to describe the wakefield effects in the counter-moving case has been developed. It was also shown that such a model is suitable both for computing the co-moving wakefield and the counter moving one. An example of application of this model has been proposed: the co-moving and counter-moving wakefield of a lossless pill box cavity has been computed. The results of the method (the wakepotential) were benchmarked against numerical simulations results with excellent agreement.

Despite the results showed in the paper are preliminary, they are really encouraging because they show that the model can correctly estimate the wakefield effects in simple systems as a pill-box cavity. Future work will develop further this model, benchmarking it against other literature results and expanding it to obtain a quantification of the RF-heating induced by two counter rotating beams circulating in the same vacuum chamber. The authors strongly believe that the application of this model could be crucial in the design of the future high intensity accelerators interaction chambers and in the design of all the components traversed by two beams.

ACKNOWLEDGEMENT

This work was partly supported by the European commission under HORIZON 2020 integrating activity project ARIES, grant agreement no 730871.

REFERENCES

[1] J. Wang, "Transverse Two-Beam Instability," CERN, Tech. Rep., 1987. https://cds.cern.ch/record/183705

[2] A. W. Chao, *Physics of Collective Beam Instabilities in High Energy Accelerators*. Wiley-VCH, 1993.

[3] K. Ng, "Physiscs of Intensity Dependent Beam Instabilities," in *U.S. Particle Accelerator School (USPAS 2002) Long Beach, California, January 14-25*, 2002. http://lss.fnal.gov/cgi-bin/find_paper.pl?fn-0713

[4] K. L. F. Bane, P. B. Wilson, and T. Weiland, "Wake fields and wake field acceleration," in *AIP Conference Proceedings*, Stanford Linear Accelerator Center, vol. 127, AIP, 1985, pp. 875–928. DOI: 10.1063/1.35182. http://aip.scitation.org/doi/abs/10.1063/1.35182

[5] O. S. Bruning *et al.*, *LHC Design Report*, ser. CERN Yellow Reports: Monographs. Geneva: CERN, 2004. DOI: 10.5170/CERN-2004-003-V-1. http://cds.cern.ch/record/782076

[6] D. Carbajo Perez *et al.*, "OPERATIONAL FEEDBACK AND ANALYSIS OF CURRENT AND FUTURE DESIGNS OF THE INJECTION PROTECTION ABSORBERS IN THE LARGE HADRON COLLIDER AT CERN," *Proceedings, 8th International Particle Accelerator Conference (IPAC 2017): Copenhagen, Denmark, May 14-19*, 2017. DOI: 10.18429/JACoW-IPAC2017-WEPVA108.

[7] L. Teofili, M. Migliorati, D. Carbajo, I. Lamas, and A. Perillo, "Design of the Target Dump Injection Segmented (TDIS) in the Framework of the High Luminosity Large Hadron Collider (HL-LHC) Project," in *61st ICFA Advanced Beam Dynamics Workshop on High-Intensity and High-Brightness Hadron Beams*, Daejeon, Korea, 2018, pp. 122–126, ISBN: 9783954502028. DOI: 10.18429/JACoW-HB2018-TUP2WE04.

[8] B. Salvant *et al.*, "BEAM INDUCED RF HEATING IN LHC IN 2015," Tech. Rep., 2016.

[9] W. Herr and T. Pieloni, "Beam-Beam Effects," *CERN Yellow Reports*, no. 1, pp. 431–459, Jan. 2016. http://arxiv.org/abs/1601.05235%0Ahttp://dx.doi.org/10.5170/CERN-2014-009.431%20http://arxiv.org/abs/1601.05235%20http://dx.doi.org/10.5170/CERN-2014-009.431

[10] C. Pellegrini, "Longitudinal Coupled Bunch Instability for Two Counterrotating Beams," CERN, Tech. Rep., 1986. http://cds.cern.ch/record/170396

[11] S. Myers, *The LEP Collider, from design to approval and commissioning*, ser. John Adams' Lecture. Geneva: CERN, 1991, Delivered at CERN, 26 Nov 1990. DOI: 10.5170/CERN-1991-008. http://cds.cern.ch/record/226776

[12] F. Zimmermann, "Two-Beam Resistive-Wall Wake Field," in *Proceedings of PAC07*, Albuquerque, New Mexico, USA, 2007, pp. 4237–4239, ISBN: 1424409179.

[13] C. Zannini, G. Rumolo, G. Rumolo CERN, and G. Iadarola, "Power loss calculation in separated and common beam chambers of the LHC," CERN, Geneva, Switzerland, Tech. Rep., 2014. https://cds.cern.ch/record/1742192/files/CERN-ACC-2014-0122.pdf

[14] G. Rumolo and C. Zannini, "Beam induced power loss with two beams," CERN, Tech. Rep., 2018. https://indico.cern.ch/event/809558/contributions/3372399/attachments/1820527/2977428/Beam_induced_power_loss_with_two_beam_review.pdf

[15] A. Grudiev, "LHC Project Note 413 Simulation and reduction of longitudinal and transverse impedances of a collimation device with two beams in one vacuum chamber," CERN, Tech. Rep., 2008.

[16] CST Solvers, *CST Solvers Website*. https://www.3ds.com/products-services/simulia/products/cst-studio-suite/solvers/

[17] W. R. Faust, "Transient behavior of a cavity," *Journal of Applied Physics*, vol. 43, no. 10, pp. 3983–3987, 1972, ISSN: 00218979. DOI: 10.1063/1.1660860.